GAS FLOW JETS TRACKING METHOD IN THE AERODYNAMICS OF AIR BREATHING ENGINES

V.M. Lapotko, Yu.P. Kukhtin, A.V.Yelanskiy, I.F. Kravchenko, Ivchenko-Progress SE, Ukraine
VMLapotko@gmail.com

The paper describes a method for tracking the jets of gas flows based on the Lagrangian-Eulerian approach usage. A system of integral equations describing q3d- flow of gas in a curvilinear coordinate system associated with the surface of the turbomachine rotation is presented, as well as a system of integral equations describing an axisymmetric swirling flow in a cylindrical coordinate system. Using the method for tracking jets of gas flows, a possibility to research a variety of unsteady processes is shown. The following phenomena are studied: the segregation phenomenon of hot and cold jets of gas on the turbine rotor blades surfaces, clocking-effect of aerodynamic interaction in the 1.5 turbine stage, determining the trajectory characteristics of unsteady gas flow in the turbine, axisymmetric swirling flow of gas in the system “engine-nacelle-external flow”.

Keywords
air breathing engines, Lagrangian-Eulerian approach

1. DESIGNATIONS

P, ρ, T – thermodynamic parameters - pressure, density and temperature;

W_m, W_φ, –velocity components in a curvilinear coordinate system;

W_x, W_r, W_φ – velocity components in a cylindrical coordinate system;

U_n – normal velocity of the contact discontinuity;

W_n – normal velocity of the gas flow;
A, V– area of surface and the amount of space;

R, C_v - gas constant, specific heat at constant volume;

$f_x^v, f_r^v, f_\varphi^v$ - volume sources, reproducing an interaction of the fan blades or outlet guide vanes with the gas flow;
m, φ - components of curvilinear coordinate system;
x, r, φ - components of cylindrical coordinate system;

$(\bar{n})_m, (\bar{n})_\varphi$ - components of the unit normal on the coordinate direction in a curvilinear coordinate system;

$(\bar{n})_x, (\bar{n})_r$ - components of the unit normal on the coordinate direction in a cylindrical coordinate system;
s, D – respectively, entropy per unit mass and additive component of the gas flow;
α – flow inlet angle;

P_a, T_a –pressure and temperature on a free boundary;
N – the number of blades in a ring;
ω – angular frequency;
k – turbulent kinetic energy;
Δt – time increment;
M – Mach number;
G – mass flow rate;
F – force acting on the blade of a turbomachine.

2. DESCRIPTION OF METHOD

In gas dynamics two approaches can be used to describe the gas flow: Eulerian approach and Lagrangian approach. Each has its advantages and disadvantages. A method, combining the advantages of both approaches could be very interesting for application [1].
In practice, this is implemented using different families of grids: the first family is a family of fixed grid surfaces, located across the flow; the second family is a family of infinitely thin moving Lagrangian surfaces, impermeable to the main flow, oriented streamwise. Given the unsteady flow, the grid surfaces of the second family should always adapt to the flow direction.
In the proposed method of calculation the values of the convection currents through the fixed grid surfaces elements for each element of space is associated with the values of movements of Lagrangian surfaces family elements in respect to the moving fluid [2]. For implementation of this corellation following conditions are required: 1) moving Lagrangian surfaces should have properties of contact discontinuity surfaces; 2) calculation of the movement of contact discontinuity surfaces and calculation of convection curents would be performed using an identical algorithm. The algorithm for solving the Riemann problem was used as such an algorithm, Fig. 1.

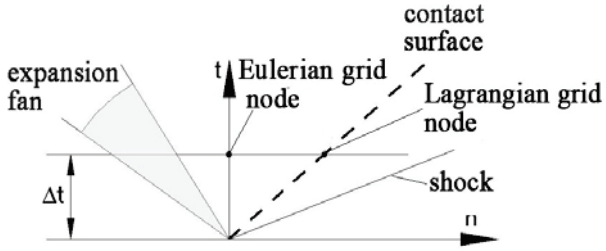

Fig. 1 Usage of the Riemann problem solution for Lagrangian-Eulerian formulation

It means that in case of fixed grid surfaces we act in the manner as the difference scheme of S.K.Godunov [3] dictates. Though in case of contact discontinuity surfaces we propose an algorithm of grid surfaces rearrangement (see Figure 2), based as well on the solution of the Riemann problem.

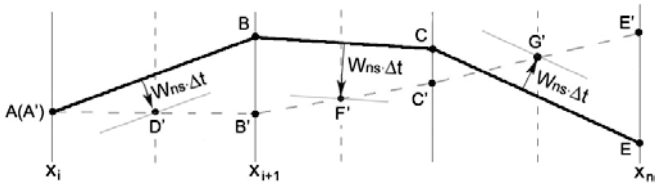

Fig. 2 Algorithm of grid surfaces rearrangement

In Figure 2 the contact discontinuity surface in timepoint t is shown as a solid line. And the contact discontinuity surface in timepoint t+Δt is shown as a dashed line.
According to the rearrangement algorithm, the initial point A´ belonging to the left boundary of the computational domain is known and in a particular case may coincide with the

initial point A of the contact discontinuity surface in a timepoint t. During the computation step Δt the AB section of the contact discontinuity surface moves to the point D with a constant velocity Wns determined from the solution of the Riemann problem, Fig. 1. In the point D, this new section is turned to align its left side with the point A´. Such turn of a new section of the contact discontinuity surface physically means that the presented algorithm takes into account the flow pre-history. Further, a new position of the point B (point B´) is determined as the intersection point of the fixed grid line X_{i+1} and a new section of the contact discontinuity surface, passing through the points A´and D´. Similar arrangements can be performed for the sections BC, CE, ... etc.

The system in Lagrangian-Eulerian representation of conservation laws of mass, momentum and energy, describing q3d flow of ideal gas in a curvilinear coordinates system (m, φ), Fig. 3,

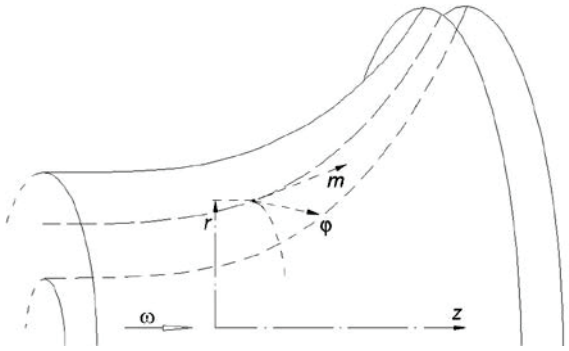

Fig. 3 Curvilinear coordinates system

associated with the rotation surface of the turbomachine, can be represented as follows:

$$\frac{\partial}{\partial t}\int_{V(t)}\rho dV = -\int_{A(t)}\rho(W_n - U_n)dA;$$

$$\frac{\partial}{\partial t}\int_{V(t)}\rho D dV = -\int_{A(t)}\rho D(W_n - U_n)dA;$$

$$\frac{\partial}{\partial t}\int_{V(t)}(\rho W_m)dV = -\int_{A(t)}\rho W_m(W_n - U_n)dA - \int_{A(t)}P(\bar{n})_m dA +$$

$$+\omega^2\int_{V(t)}\rho r\frac{\partial r}{\partial m}dV + 2\omega\int_{V(t)}\rho\frac{\partial r}{\partial m}W_\varphi dV + \int_{V(t)}\rho\frac{1}{r}\frac{\partial r}{\partial m}W_\varphi W_\varphi dV; \quad (1)$$

$$\frac{\partial}{\partial t}\int_{V(t)}(\rho(rW_\varphi))dV = -\int_{A(t)}\rho(rW_\varphi)(W_n - U_n)dA - \int_{A(t)}rP(\bar{n})_\varphi dA -$$

$$-2\omega\int_{V(t)}\rho r\frac{\partial r}{\partial m}W_m dV;$$

$$\frac{\partial}{\partial t}\int_{V(t)}(\rho E)dV = -\int_{A(t)}\rho E(W_n - U_n)dA - \int_{A(t)}PW_n dA +$$

$$+\omega^2\int_{V(t)}\rho r W_m\frac{\partial r}{\partial m}dV,$$

where: $E = C_V T + \frac{W^2}{2}$; $P = \rho RT$

The resulting difference scheme provides high effectiveness and accuracy of the solution. The computation of all parameters and grid coordinates takes place in a single pass over the space. In other words the position and motion of Lagrangian surfaces are continually uniformly linked with the change of parameters in space.

The described strategy is a kind of development of S.K.Godunov method for the Lagrangian-Eulerian representation. When we consider the flow of gas on the steady state, the Lagrangian surfaces behave as current surfaces and the fluid enclosed between the Lagrangian surfaces represents the strem tube. However, when considering the unsteady flows, such concepts as the current surfaces and the stream tubes are not correct. Therefore, regardless of the flow regime, we use such concepts as surfaces of flow jets and flow jets.

In all presented calculations, the heat and mass transfer phenomena caused by the physical viscosity and turbulent motion of the gas was simulated using the streams of gasubstance between adjacent volumes of space [4]. In this case the system of equations (1) was supplemented with the terms containing the sources or sinks of mass, momentum and energy. Due to the limited amount of represented material, heat and mass transfer model is not considered here.

The formulation of boundary conditions did not differ from the formulation described in the paper [3].

All values involved in calculations were reduced to a dimensionless form. An axial length of the computational domain was taken as a reference length. An isothermal speed of sound, defined by the parameters at the output of the computational domain, served as a reference velocity. Pressure and temperature were reduced to a dimensionless form through the appropriate values of parameters at the output of the computational domain.

3. SEGREGATION OF HOT AND COLD JETS OF GAS ON THE SURFACES OF TURBINE BLADES

A common scheme for calculating the flows in multi-stage turbomaschines is the use of local coordinate systems in the fixed and rotating blade rows. Established method in construction of numerical scheme for interface between fixed and rotating blade rows is the use of sliding grids. In the case of high rotor speed Wx/Wφ<0.5, there is a "smearing" of the flow parameters at the interface of grids, Fig. 4.

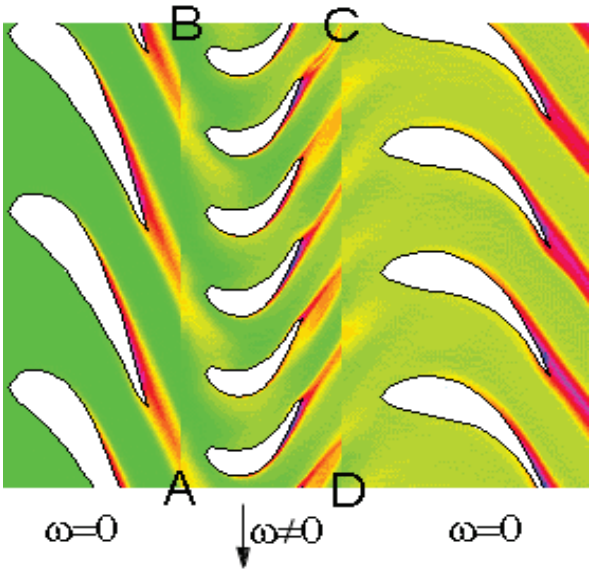

Fig. 4 Calculation of q3d unsteady flow in 1.5 turbomachinery stage using sliding grids, (entropy field)

The reason for this negative phenomenon is the use of different coordinate systems in the moving and fixed grids. To eliminate it, the flow in the turbine wheel was calculated in the absolute coordinate system.

In this coordinate system when the jets get onto the wheel

blades, their fragmentation or splitting into segments occurs, Fig. 5. While the individual segments of jets pass through the blade passages they are deformed and reoriented in space. After passing the blade passages, the jet segments are not joined at the outlet of the blade passages, and slide along the wakes (surfaces) going down from the blades trailing edges.

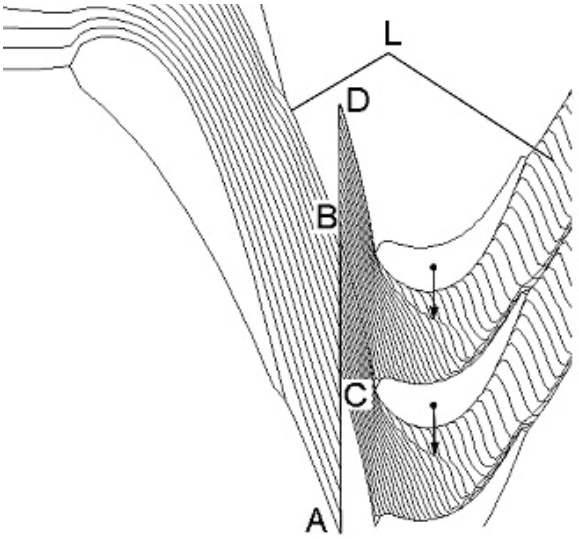

Fig. 5 Lagrangian grid lines field in turbomaschine stage

With the same calculation scheme, a key unresolved task was the problem of calculating the phenomenon of flow jets separation at the surfaces of the rotor blades. This problem had been successfully resolved. In a later version the start and end points of the flow jets segments may slide over the surfaces of adjacent jets in their relative movement, Fig. 6.

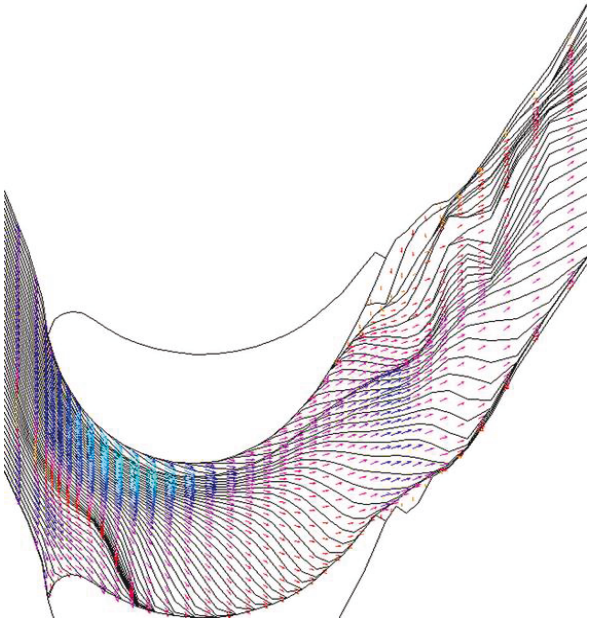

Fig. 6 The structure of the grid lines and the velocity vector field in a new version of the algorithm

This improvement allowed us to calculate the segregation process of hot and cold jets of gas on the surfaces of turbine rotor blades. This phenomenon is characterized in the following:

1) high-speed jets of the flow core displace the wakes of the nozzle guide vanes near the pressure surface of the rotor blade;
2) and vice versa, the wakes of the nozzle guide vanes displace the high-speed jets of the flow core near the suction surface of the rotor blade, Fig. 7, [5].

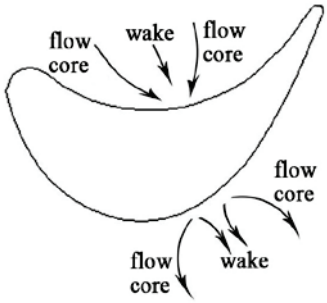

Fig. 7 The phenomenon scheme of flow jets displacement near the surfaces of the rotor blade:

In the case of film cooling of the nozzle guide vanes the wakes carry the cold air. If there is a nonuniformity of temperature in the combustion chamber, flow core jets usually carry hot gas, Fig. 8.

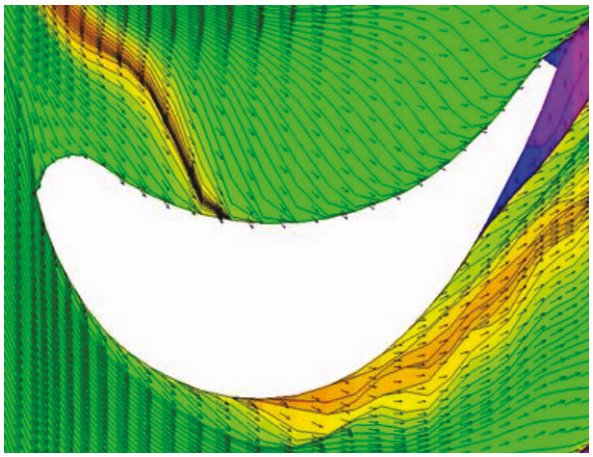

Fig. 8 Fragment of the entropy field, velocity field and flow jets near the surfaces of the rotor blade

Then, as a result of the segregation process, heating of the pressure and cooling of the suction surface of the rotor blade will take place. That can cause adverse thermal stresses of the blade airfoil [6].
Experimental and computational studies implemented in similar conditions have shown that gas layers close to the pressure surface of the rotor blade have a higher stagnation temperature (by 50 - 150^{0}C) than the corresponding gas temperature close to the suction surface.

4. ANALYSIS OF CLOCKING – EFFECTS IN THE 1.5 STAGE OF GAS TURBINE

Unsteady flow in turbomachines becomes more ordered, when there are non-adjacent blade rows with the same or multiple number of blades. Taking these ordered flow structures into account, it is possible to significantly improve some characteristics of the turbomachines.
The object of numerical studies was 1.5 turbine stage, geometric and aerodynamic parameters of which, as well as the results of experimental measurements, were taken from the paper [7], Fig. 9.

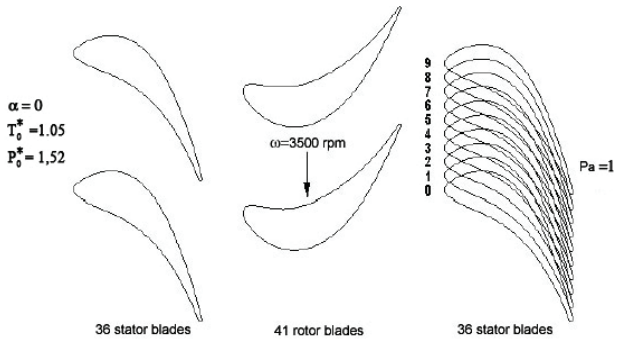

Fig. 9 Investigated 1.5 stage of low-pressure turbine

The calculation results show that when the stators are in position "0" there is a weak interaction between the first stator wakes and the second stator airfoils, Figs. 10 -11. This interaction is characterized by the first stator wakes passing inside the second stator blade passages. At the same time in the position "4", after the blade ring has passed, first stator wakes are getting on the second stator airfoils, causing an increase in turbulent kinetic energy and gas flow entropy, Figs. 12 -13. This adversely affects the turbine efficiency.

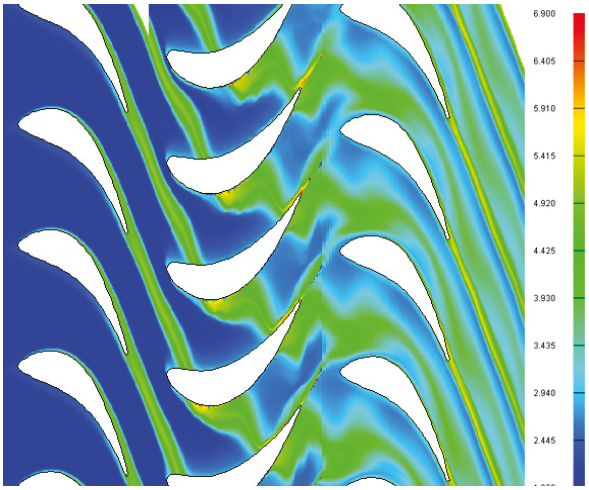

Fig. 10 Fragment of the instantaneous flow field in turbine for the relative position "0" of stators, $k_{T^*}1000$ parameter

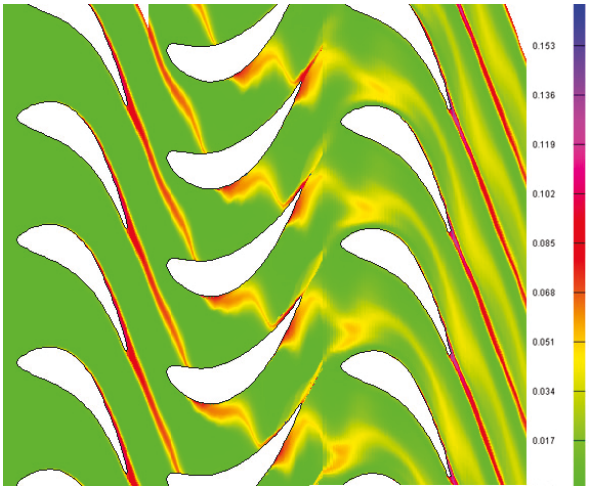

Fig. 11 Fragment of the instantaneous flow field in turbine for the relative position "0" of stators, s parameter

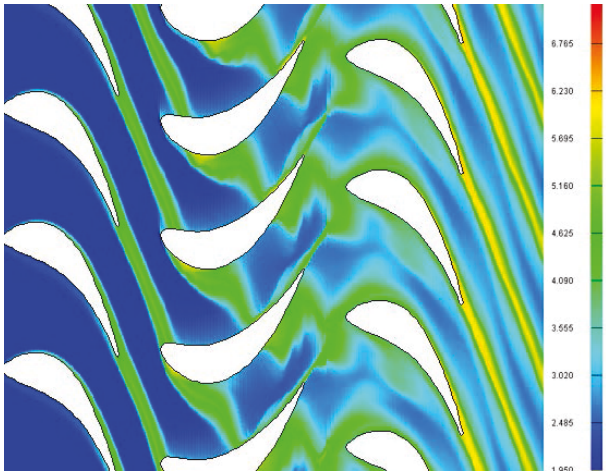

Fig. 12 Fragment of the instantaneous flow field in turbine for the relative position "4" of stators, $k_{T^*}1000$ parameter

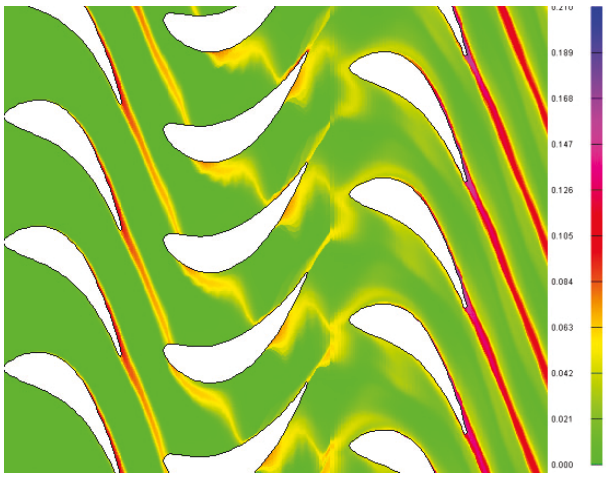

Fig. 13 Fragment of the instantaneous flow field in turbine for the relative position "4" of stators, s parameter

The relative end absolute values of the 1.5 turbine stage efficiency for all relative orientations of stators, obtained by calculation are shown in Fig. 14 [8]. There are also the experimental values taken from the paper [7].

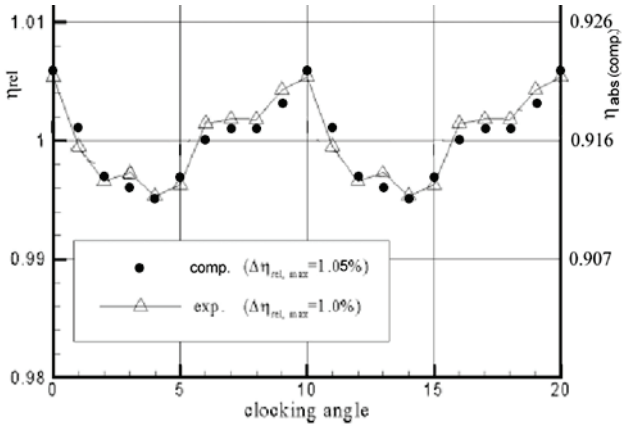

Fig. 14 Relative end absolute values of turbine efficiency when changing the relative orientation of stators

Rotor blade is subjected to the periodic influence from the viscous wakes and the potential effects, caused by the stationary stator grid. This method let us solve the task of the optimization of the mutual stator grid orientation with the aim to reduce the exciting load amplitude, which results in vibration of the rotor blade. However, to make Fourier analysis of the exciting load, the execution of the long (1.5-2 rotor turns) calculations of the entire turbine with different stator orientation is needed.

Calculations, made for “0”, “2”, “4”, “6”, and “8” locations of the nozzle block 2 showed that “2” and “6” position of the nozzle block 2 have very interesting results in the sense of extreme dynamical loads generation, acting on the rotor blade. It is a result of the Fourier analysis of the time change of the axial, Figs. 15, 16 and circumferential, Figs. 17, 18 force components and also torsional moments, Figs. 19, 20, acting on the rotor blade.

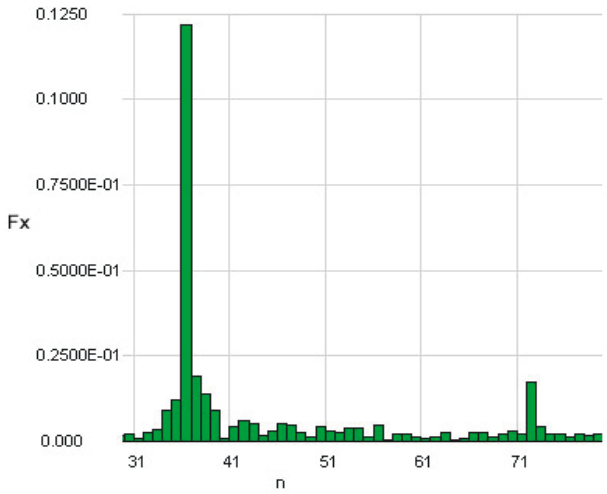

Fig. 15 Fourier analysis of the axial force component, acting on the rotor blade for the relative position "2" of stators

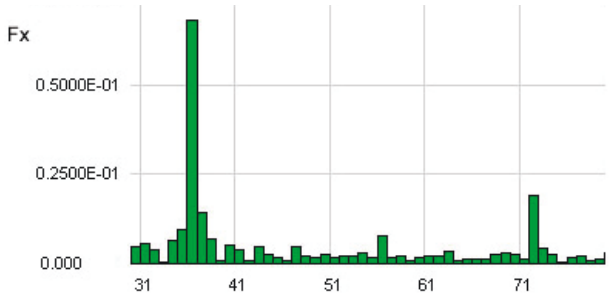

Fig. 16 Fourier analysis of the axial force component, acting on the rotor blade for the relative position "6" of stators

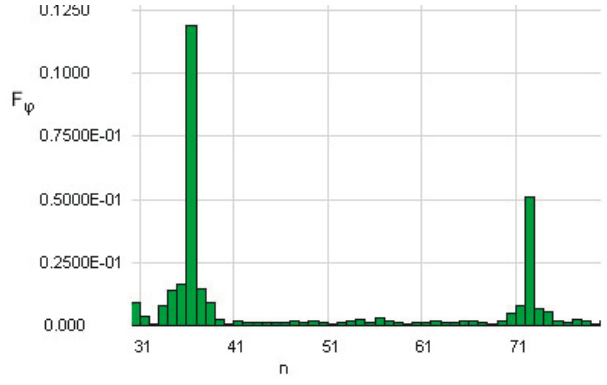

Fig. 17 Fourier analysis of the circumferential force component, acting on the rotor blade for the relative position "2" of stators

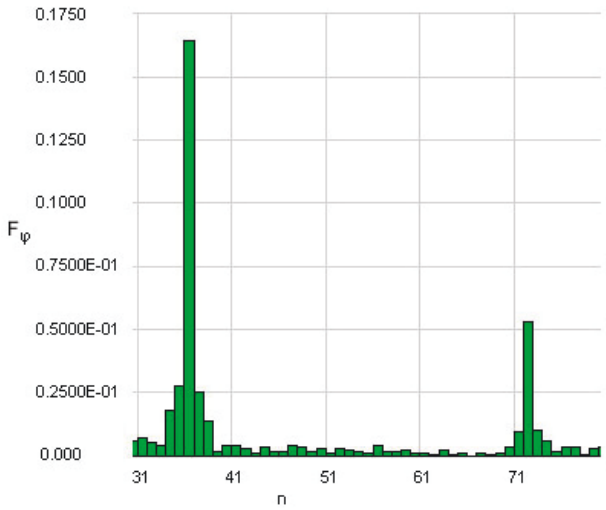

Fig. 18 Fourier analysis of the circumferential force component, acting on the rotor blade for the relative position "6" of stators

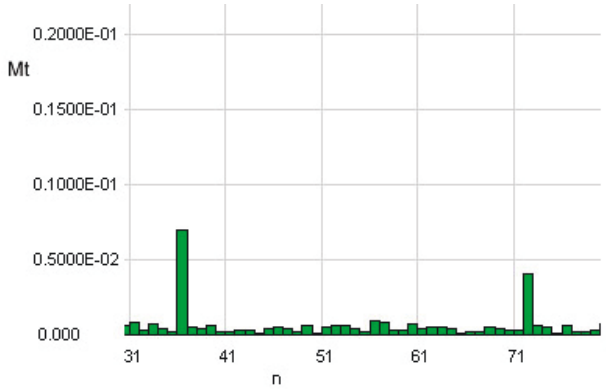

Fig. 19 Fourier analysis of the torsional moment, acting on the rotor blade for the relative position "2" of stators

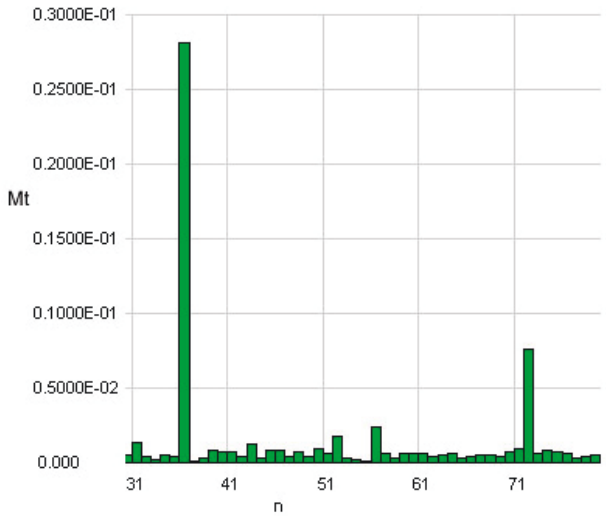

Fig. 20 Fourier analysis of the torsional moment, acting on the rotor blade for the relative position "6" of stators

Here we must take into account, that in position “6” of stators, Fig. 18, there is a biggest circumferential force component Fφ, with minimal axial load Fx, Fig. 16. However, in position “2” of stators there is a minimal torsional moment Mt, Fig. 19, of the rotor blade relative to the blade axis.

5. DETERMINATION OF THE TRAJECTORY CHARACTERISTICS OF UNSTEADY GAS FLOW IN THE AIRCRAFT ENGINE TURBINE

There are various starting systems of turbojet engine afterburners. Among these systems, the afterburner ignition system according to the “fiery path” method occupies a special place. This system provides high reliability of ignition, minimizes the starting afterburner fuel flow rate, reduces startup time of afterburner [9].
The operating principle of such a system is based on the short-time injection of additional fuel into the main combustion chamber at startup. The fuel-air jet formed by a spray atomizer extends along the turbine duct to the afterburner flame stabilizer. At the turbine outlet a jet of such "fiery path" creates favorable conditions for reliable ignition of the afterburner fuel-air mixture.
The specifics of the given task was to determine the optimal trajectory of the fuel-air jet, extending from the combustion chamber to the afterburner flame stabilizers. Therefore the unsteady flow in the turbine, consisting of 5 full rings, was calculated as a whole, see Fig. 15.

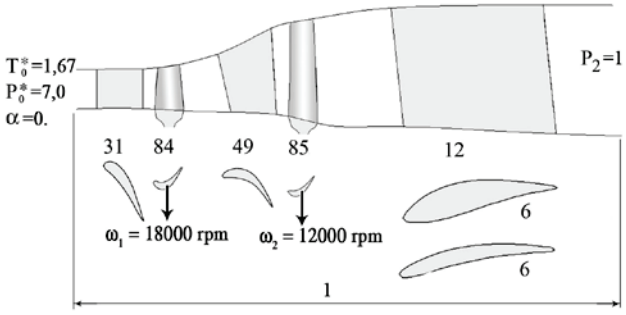

Fig. 15 Flow path and schematic view of the turbine

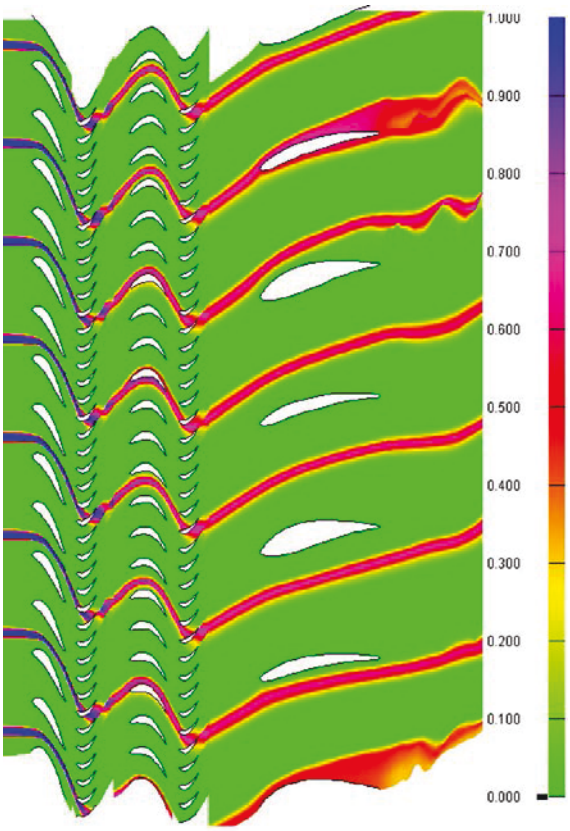

Fig. 16 Fragment of unsteady flow field of additive component in the turbine

We assumed that a full fuel evaporation occurred in front of the first nozzle guide vanes blade passage. The processes of fuel combustion were not simulated. In this formulation, the propagation of burning fuel jets can be simulated with the propagation of gas jets consisting only of the gas flow additive component. D=1.0 on the left boundary.
As an example, Figs. 16 and 17 show a fragment of unsteady gas flow in the turbine. It can be seen that not all possible positions (in this case there are 31 of them) of "fiery path" are acceptable for a favorable propagation of the fuel-air jet. Due to the interaction with some elements of the turbine duct some "fiery path" can be substantially dispersed. Some of the "fiery path" can cause overheating of the individual turbine parts during continuous fuel injection. The angular displacement of the acceptable fuel-air jet made up ≈ 16^0 in a direction opposite to the direction of the rotors rotation.

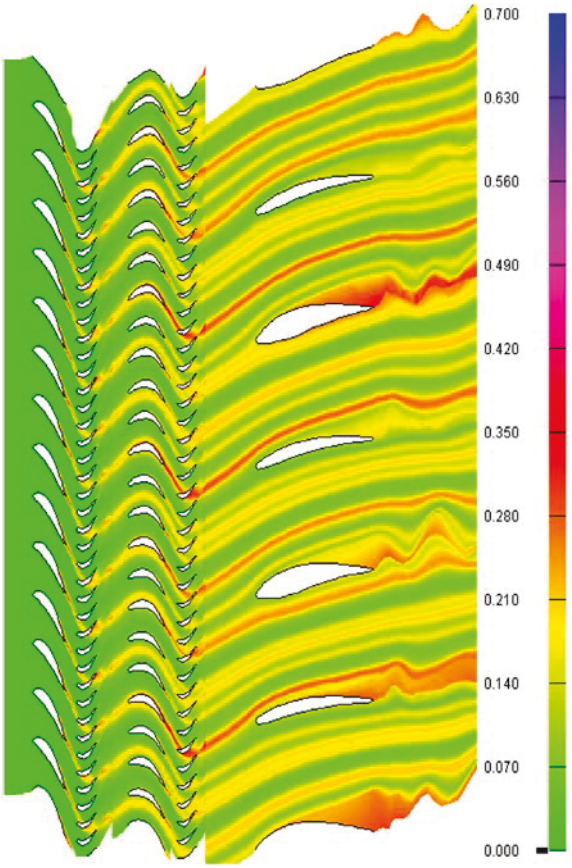

Fig. 17 Fragment of unsteady flow field of entropy per unit mass in the turbine

Experimental determination of the spatial orientation of the "fiery path" along the gas flow duct of a modern turbofan is associated with methodological difficulties and high material costs. However, despite the absence of obtained design data verification, these results were takes as a basis of the initial data in the design of such systems.
Reliable, stable start of the afterburner ignition system in the early design stages indirectly confirmed the correctness of the design procedure.
Only 2 years after the beginning of research, reliable experimental data were obtained through a random failure of the automatic fuel control system of the test bench. Failure of the fuel cut-off in a spray atomizer within a period that was significantly higher than the permissible time has

caused the formation of a well visible wakes in areas of cooling air blowing along the gas flow duct outer contours.
Fig. 18 shows a comparison of the design configuration of the "fiery path" (shown by a wide continuous strip) with visually recorded places of severe exposure to high-temperature flame with the gas flow duct outer contours (shown with "*" symbol).

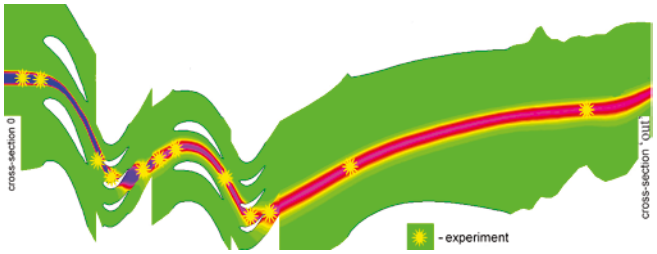

Fig. 18 The results of comparison between the design data and the experiment

6. CONJUGATE GAS-DYNAMIC MODEL OF THE BYPASS DUCT AND THE OUTER PART OF THE TURBOFAN NACELLE [10]

In the development of the present gas-dynamic model it was assumed that the gas flow in the under consideration technical devices can be well described as an axially symmetric, swirling flow in the Lagrangian-Eulerian form of representation. The gas flow within the bypass duct, the flow from the outside of the nacelle, as well as the flow at the inlet and outlet of the main duct of a turbofan, are considered as a unit unsteady dynamic process.
In the proposed gas-dynamic model the momentum and energy input occurring during the fan impeller rotation were taken into account. The process of energy conversion that takes place in the area of the outlet guide vanes location was also taken into account. These processes were reproduced with volume sources $f_x^v, f_r^v, f_\varphi^v$ - the intensities of which were obtained by considering the interaction of the impeller blades and the outlet guide vanes with axially symmetric, swirling gas flow.
Given these assumptions, the basic system of equations for the gas flow without viscosity in a cylindrical coordinate system (x, r, φ) is represented as:

$$
\begin{aligned}
&\frac{\partial}{\partial t}\int_{V(t)}\rho dV = -\int_{A(t)}\rho\left(W_n - U_n\right)dA\,,\\
&\frac{\partial}{\partial t}\int_{V(t)}\rho W_x dV = -\int_{A(t)}\rho\left(W_n - U_n\right)W_x dA - \int_{A(t)}P(\vec{n})_x dA + \int_{V(t)}f_x^V dV\,,\\
&\frac{\partial}{\partial t}\int_{V(t)}\rho W_r dV = -\int_{A(t)}\rho\left(W_n - U_n\right)W_r dA - \int_{A(t)}P(\vec{n})_r dA + \\
&\qquad + \int_{V(t)}\rho\frac{W_\varphi^2}{r}dV + \int_{V(t)}f_r^V dV\,,\\
&\frac{\partial}{\partial t}\int_{V(t)}\rho\left(W_\varphi r\right)dV = -\int_{A(t)}\rho\left(W_n - U_n\right)\left(W_\varphi r\right)dA + \int_{V(t)}f_\varphi^V r dV\,,\\
&\frac{\partial}{\partial t}\int_{V(t)}\rho\left(C_V T + \frac{W^2}{2}\right)dV = -\int_{A(t)}\rho\left(W_n - U_n\right)\left(C_V T + \frac{P}{\rho} + \frac{W^2}{2}\right)dA + \\
&\qquad + \int_{V(t)}\left(f_x^V W_x + f_\varphi^V W_\varphi + f_r^V W_r\right)dV\,,\\
&P = \rho R T\quad .
\end{aligned}
\tag{2}
$$

In the numerical implementation of the proposed model, great attention was paid to the effectiveness of made calculations and to the possibility to perform a rapid adaptation of the model to a specific engine. With this object in mind, the computational domain was divided into several sub-areas, which contained definite components of the engine and the nacelle. These sub-areas can be processed on a parallel computer system at a given moment of time, independently of each other (see Fig. 10).

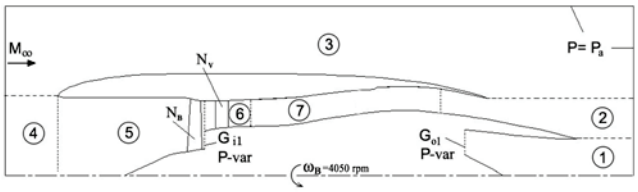

Fig. 19 Block structure of the computational domain

As the initial geometric parameters in the considered model, besides the gas flow duct contours, the geometric shapes of the 20 fan blades airfoils and of the 52 outlet guide vanes airfoils shall be determined.
At the surface of the main duct inlet the absolute parameters and the flow inlet angle were set. Static pressure was chosen to obtain a given flow rate G_{i1}.
At the surface of the main duct outlet the absolute parameters, as well as the flow angle were set. Static pressure varied to ensure the flow rate G_{s1}.
The fan operation was determined by the angular frequency ω_B=4050 rpm. Flight Mach number – 0.8, cruising flight altitude – 11km.
The developed mathematical model was verified by the integral parameters, known from experimental data of existing engines, as well as from the parameters obtained using other mathematical models.
Numerical investigations were performed, to find the optimal aerodynamic shapes of the engine, nacelle and pylon. The criteria for assessing the quality of the design were the lack of shock waves and separated zones and ensuring of maximum power plant thrust in cruising regime.
All the jet thrust values were reduced to the ideal thrust value that was calculated based on the full gas parameters after the outlet straightener blades, and on the flight conditions.
Figures 20 - 23 present the field of the contact discontinuity surfaces, as well as the parameters fields, formed on the steady-state gas flow in the initial profile of the engine-nacelle system.
On the outer side of the air intake lip, as well as on the outer side of the bypass duct nozzle casing, presence of supersonic zones can be seen.

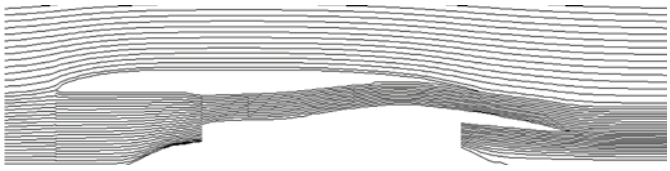

Fig. 20 Family of the Lagrangian (contact discontinuity) surfaces on steady-state flow

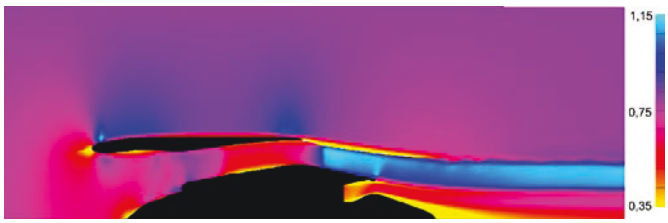

Fig. 21 Distribution of the dimensionless speed M

Fig. 22 Distribution of total pressure

Fig. 23 Distribution of velocity circumferential component

After changing the outer and inner contours of the nacelle, reprofiling of the air intake and the main duct exhaust nozzle, significant changes of the flow field have occurred in the system, see Fig. 24 - 26. The available thrust of the consideration engine increased in 1.16 times.

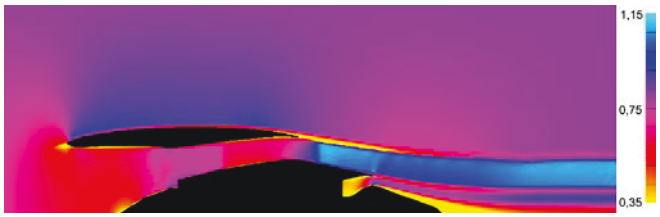

Fig. 24 Distribution the dimensionless speed M

Fig. 25 Distribution of total pressure

Fig. 26 Distribution of turbulent kinetic energy *1000

Aerodynamic processes in the engine can evolve in time when the fan impeller speed changes, the fan and the outlet guide vanes geometry changes, the exhaust nozzles configuration changes, as well as when the flight conditions change. The represented method for calculating gas flow in time allows to study the unsteady gas-dynamic processes.

7. NUMERICAL EVALUATION OF THE TONAL NOISE LEVEL IN THE SOURCE UNDER UNSTEADY INTERACTION OF TURBOMACHINES BLADE ROWS [11]

Taking into account the three-dimensionality of the geometry of researched objects, as well as the spatial character of parameters distribution at the inlet of the computational domain, Fig. 27,

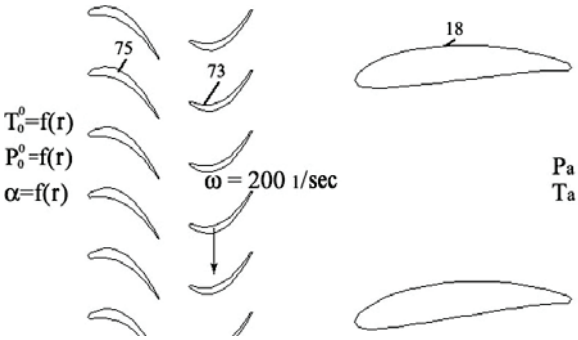

Fig. 27 The computational domain scheme

the proposed calculation method was modified. Now, several computational layers can be located along the radius; the positions of their boundaries are set based on the preliminary solution of the numerical definition problem of the axial-radial gas flow in the Lagrangian-Eulerian formulation, see Fig. 28.

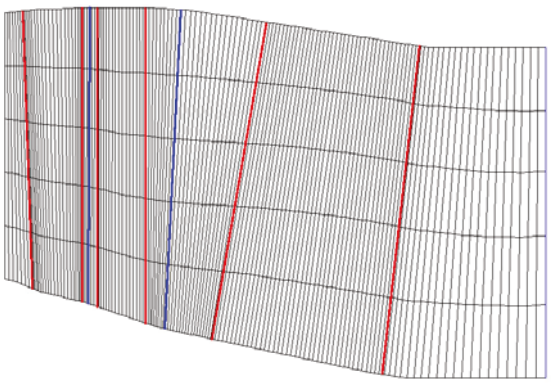

Fig. 28 Schematic meridional view of the turbine with computational grid layers

When performing the basic calculation, the position of the computational layer boundaries remains unchanged. Of course, such formulation presupposes the absence of significant secondary flows.

As a result of aerodynamic calculations of the whole turbine the parameter fields have been obtained within several rotations of the rotor, for example, see Fig. 29. An analysis of these fields has shown that after the first nozzle guide vanes there are aerodynamic wakes characterized by a velocity defect and a practical lack of nonuniformity in pressure and in orientation angle of the velocity vectors, see Fig. 30. At the same time, after the turbine wheel blades aerodynamic wakes are formed, characterized by a slight velocity defect, a practical lack of nonuniformity in pressure and a strong change (10 -15 °) in the orientation angle of the velocity vectors, see Fig. 31.

It is known that the tonal noise occurrence is caused by periodic pressure pulsations on the surfaces of the blades resulting from the impact of aerodinamic nonuniformities of the flow on them.

Such pressure fields at all points of the blades surfaces accumulated over the calculation time in the course of 1.5-2.0 rotations of the rotor. The results of the Fourier analysis of obtained fields are shown in Fig. 32, 33.

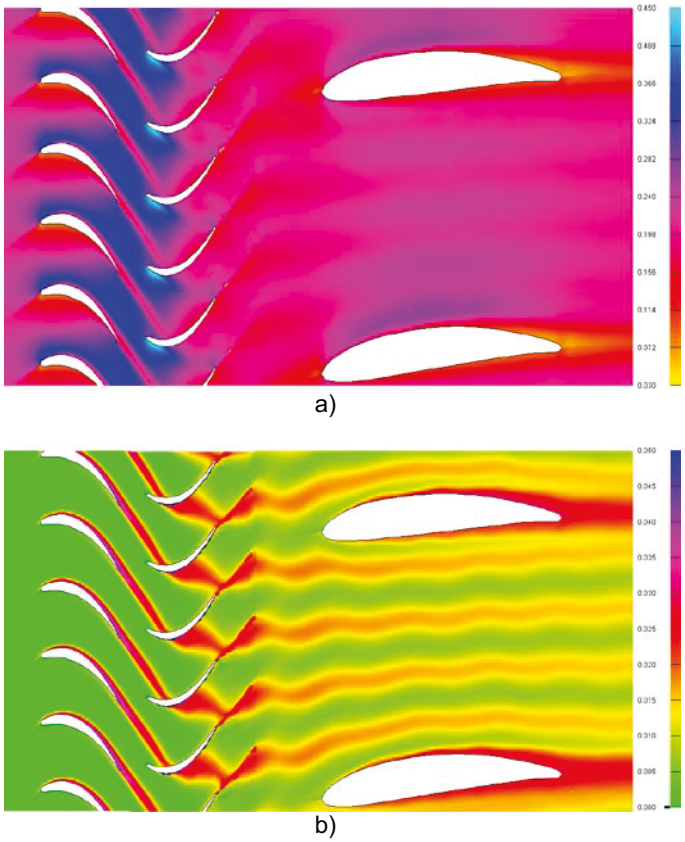

a) b)

Fig. 29 Fragments of the instantaneous parameter field for the middle computational layer:
a) M number; b) entropy

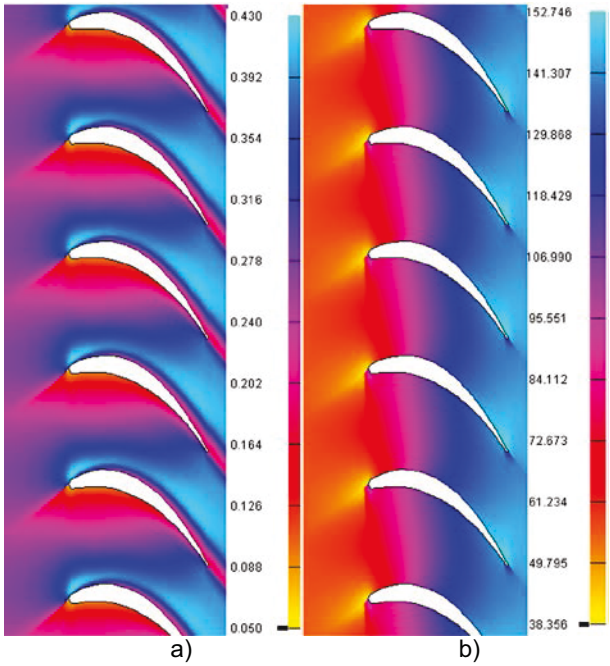

a) b)

Fig. 30 Fragments of instantaneous fields:
a) M number; b) velocity vectors angles

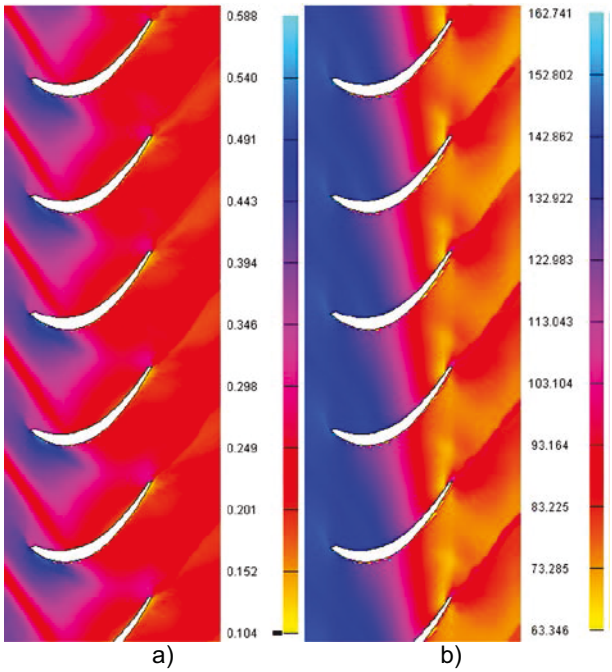

a) b)

Fig. 31 Fragments of instantaneous fields:
a) M number; b) velocity vectors angles

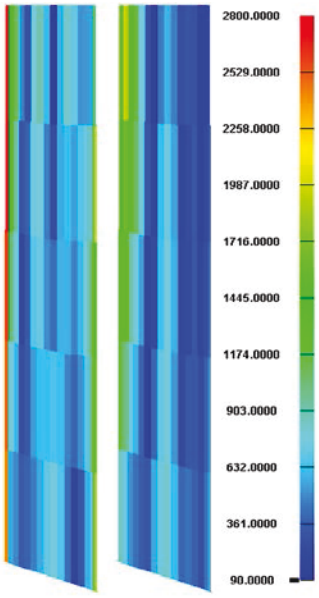

a) b)

Fig. 32 Distribution of the pulsation pressure of the 75th harmonic over the surface of the blade:
a) pressure side; b) suction side

These figures show that as a result of the aerodynamic wakes interaction with downstream surfaces, the largest pressure pulsations are observed at the leading edges of the rotor blades and airfoils. However, in addition, the areas of intense pressure pulsation are observed at the lateral surfaces of the airfoils at a distance of 30% from the root section. It is caused by the flow separation, see Fig. 34.
The pulsation pressure fields obtained this way can be used to calculate the acoustic characteristics of the flow. They characterize the level of aerodynamic noise in the source.

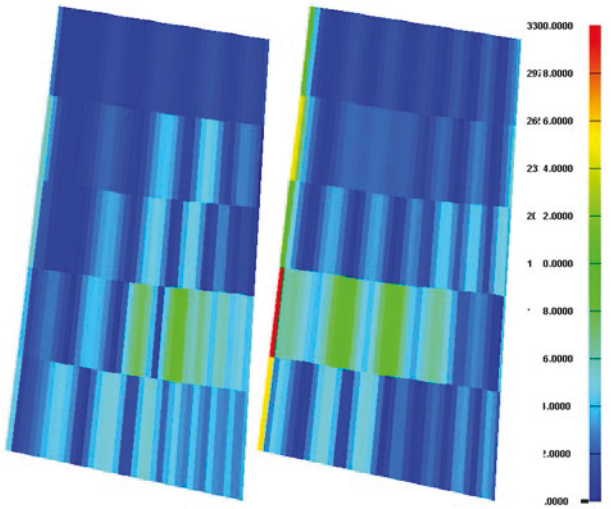

a) b)

Fig. 33 Distribution of the pulsation pressure of the 73th harmonic over the surface of the airfoil:
a) pressure side; b) suction side

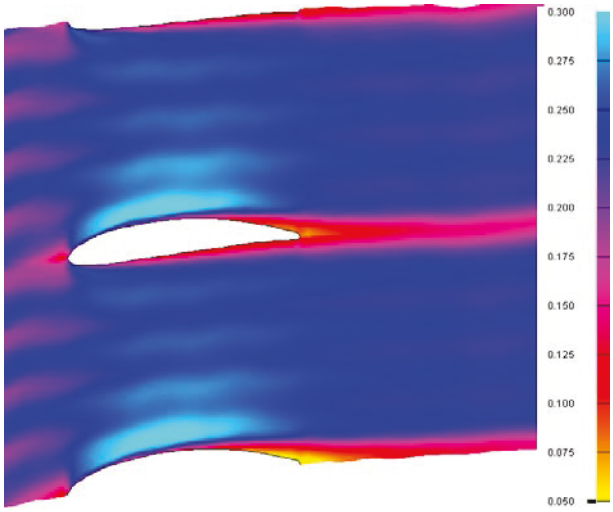

a)

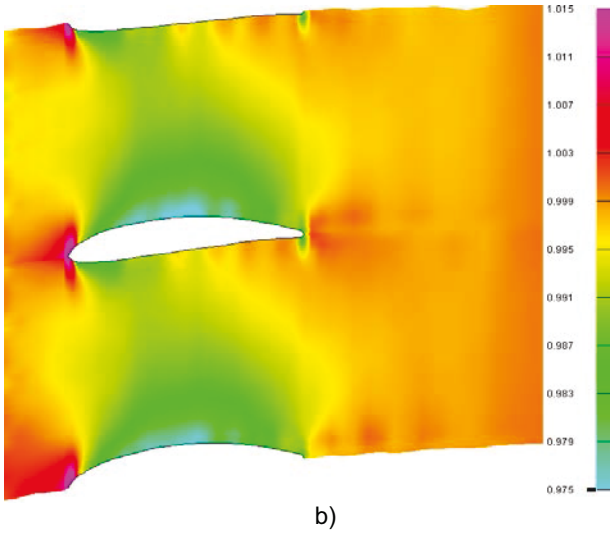

b)

Fig. 34 Flow structure in the area of flow separation near the struts airfoils surfaces: a) M parameter; b) static pressure

8. CONCLUSIONS

Years of experience in the aircraft engines design bureau has shown a high efficiency of using this approach in the design and development of various aerodynamic systems.

LITERATURE

1. V.M. Lapotko, Yu.P. Kukhtin, The advantages of using moving, Lagrangian grids for the numerical simulation of flows of the continua// Aerospace Engineering and Technology: Edited volume. - Kharkiv: KhAI, 2000.-No. 19. Thermal engines and power plants, p. 88-92. (in Russian)

2. J. Brackbill, Numerical magnetic hydrodynamics // Computational methods in physics. Controlled thermonuclear fusion.- M: Mir, 1980, p. 11-50. (in Russian)

3. S.K. Godunov, A.V. Zabrodin, M.Ya. Ivanov, A.N. Kraiko, Numerical solution of multi-dimensional problems of gas dynamics. – M.:Science, 1976. – 400p. (in Russian)

4. D.A. Munshtukov, V.M. Lapotko, Model of the fluid turbulent motion. Kharkiv 1989. depos. in VINITI 22.07.1989 No. 7158-B89. (in Russian)

5. V.M. Lapotko, Yu.P. Kukhtin, Ya.I. Bliumin, Segregation of gas flows in axial turbomachinery, and the problem of providing a uniform thermal loading of turbine rotor blades// Aerospace Engineering and Technology. No. 23. Engines and power plants, Kharkiv: KhAI, 2001.- p. 28-32. (in Russian)

6. V.M. Lapotko, Yu.P. Kukhtin, Numerical simulation of turbine blades film cooling in an unsteady gas flow// Engine technology reporter. No.3, Zaporozhye: Motor-Sich JSC, 2005, p. 90-97. (in Russian)

7. Volmar, T., Brouillet, B., Benetschik, H., Gallus H.E.: Test Case 6: 1-1/2 Stage Axial Flow Turbine – Unsteady Computation, in: ERCOFTAC Turbomachinery Seminar and Workshop. (1998).

8. V.M. Lapotko, Yu.P. Kukhtin, A.V. Lapotko, A full analysis of the Clocking-effects in the 1.5 stage of gas turbine using the method for tracking the jets of gas flows// Engine technology reporter. No.2, Zaporozhye: Motor-Sich JSC, 2011, c. 14-19. (in Russian)

9. I.F. Kravchenko, V.M. Lapotko, Yu.P. Kukhtin, Determination of the trajectory characteristics of unsteady gas flow in the aircraft engine turbine// Aerospace Engineering and Technology, No.10/57, Kharkiv: KhAI, 2008, c. 93-95. (in Russian)

10. V.M. Lapotko, Yu.P. Kukhtin, A.I. Popuga, A.V.Yelanskiy, Gas Flow Modeling in the Engine-Nacelle-Aircraft Pylon System. Proceedings, The 22nd ISABE Conference, Session 47: Fluid&Gas Dynamics, 5p. /October 25-30, 2015 Phoenix, AZ USA

11. V.M. Lapotko, Yu.P. Kukhtin, G.I. Slynko The method of numerical evaluation of the tonal noise level in the source under unsteady interaction of tubomachines blade rows. // Aerospace Engineering and Technology. No. 8(95), Kharkiv: KhAI, 2012, p.184 - 189. (in Russian)